Jia et al., J Material Sci Eng 2018, 7:5
DOI: 10.4172/2169-0022.1000486

Journal of Material Sciences & Engineering

Research Article Open Access

Research on Shear Horizontal Waves in Bars of Rectangular Cross-Section

Jia JH*, Liao ZY, Lv ZZ, Tu Y and Tu ST

Department of Mechanical and Power Engineering, Key Laboratory of Pressure Systems and Safety, Ministry of Education, East China University of Science and Technology, Shanghai, 200237, PR China

Abstract

Shear horizontal (SH) waves are increasingly popular in structural health monitoring, which can purely propagate in waveguide bars of rectangular cross-section. This kind of bars is a crucial medium to monitor the components working in harsh environments, so that the sensing part is not influenced by environments. In the present study, the wave propagation equation of SH waves propagating in waveguide bars of rectangular cross-section is derived theoretically. The equation depicts that the SH waves can go through rectangular cross-section waveguide bars just like how they propagate in an infinite plate. Influences of structural sizes of waveguide bars on wave propagation are analyzed by ANSYS simulation and experiments. Experiment results are in excellent agreement with the simulation values. Moreover, results indicate that the waves distribute equally along the thickness section. And when the width of the bar is six times wider than the wavelength, there is only the fundamental SH wave excited and it propagates clearly in a non-dispersive way. The conclusions can supply a reliably methodology for the application of SH waves in bars of rectangular cross-section.

Keywords: Waveguide bar; Fundamental shear horizontal wave; Propagating mechanism; Rectangular Cross-section; Non-dispersion

Introduction

The structural health monitoring of components with permanently installed transducers is a useful way to maintain their safety [1-3]. Moreover, guided wave technique is a reliable non-destructive testing technique [4-10]. When an appropriate waveguide bar is used to transmit waves, the guide wave technique could be a possible method for monitoring components working in high temperature environment, because the sensing parts of transducers cannot be influenced by the hostile environment on this condition. In order to extend the application of the ultrasonic guided waves technique into high temperature components, several kinds of waveguide bars have been introduced. The waveguide rods have been analyzed and been used in numerous NDE applications [11-14]. A spiraled sheet to measure flow of a hot fluid in a pipe has been proposed by Heijinsdijk et al. [15]. A bundle of thin wires have been applied to effectively suppress wave dispersion by Lynnworth et al. [16]. The tapered waveguide has been investigated numerically and experimentally by Kwon et al. [17]. Large aspect ratio rectangular strips have been researched by Cegla and Jia et al. [18-20]. According to the above-mentioned researches, it is clearly known that different shapes of waveguide bars can transmit different modes of guided waves to achieve different design purposes. Among of them, the research of waveguide strips is the most promising [18,19]. Cegla et al. have applied strips as waveguide bars to measure high temperature component. However, they haven't analyzed the propagating mechanism in strips, which is a relatively long narrow piece of plate. Jia et al. have discussed the width criteria of bars made of 316L stainless steel. Nevertheless, the conclusion can't be extended to the bar made of other material.

About waves existing in plates, there is a set of shear horizontal (SH) waves in addition to the Lamb wave modes. The polarized direction of SH modes is parallel to the surfaces of the plate and there is no out-of-plane particle displacement, so it is less affected by the presence of surrounding media [18]. Therefore, SH waves are increasingly popular in structural health monitoring and several efforts have been made about the excitation of SH waves recently. Kamal and Giurgiutiu have discussed the excitation of SH waves with shear type piezoelectric wafer active sensor [21]. Köhler et al. have proposed a piezoelectric fiber patch transducer for excitation of SH waves [22]. Seung et al. have put forward a new electromagnetic acoustic transducer to generate omnidirectional SH guided waves in metallic plates [23]. Zhou et al. have presented guided wave generation, sensing, and damage detection in metallic plates using SH waves [24]. Miao et al. have depicted d_{24} and d_{36} type transducers to excite fundamental SH wave (shorten for SH0 wave) [25,26].

The successful excitation of the SH waves is of great engineering significance. However, it's a pity that these methods can't be put into use in high temperature environment. Therefore, the design of suitable waveguide bars to introduce SH waves into harsh environment application is very important in real engineering of aerospace and process industries. According to the vibration characteristics of the SH waves in plates, the waveguide bar of rectangular cross-section is a preferred shape. Waves in bars of rectangular cross-section have been researched by Mindlin and Fox [27]. They found an exact solution of the equation for a family of wave modes in an infinite bar of rectangular cross section for certain ratios of width to depth. Because the solution is too complex, it is too difficult to be used to design suitable waveguide bars for propagating SH waves into components in harsh environment. In order to design preferred waveguide bars for high temperature application, it is vital to research the propagating mechanism of SH waves in waveguide bars of rectangular cross-section, which can provide important theoretical methodology for the design of waveguide bars.

Therefore, the propagating mechanism of SH waves in waveguide bars of rectangular cross-section is analyzed in the present research.

***Corresponding author:** Jia JH, Department of Mechanical and Power Engineering, Key Laboratory of Pressure Systems and Safety, Ministry of Education, East China University of Science and Technology, Shanghai, 200237, PR China, Tel: 86-64251834; E-mail: jhjia@ecust.edu.cn

Received August 29, 2018; **Accepted** September 11, 2018; **Published** September 21, 2018

Citation: Jia JH, Liao ZY, Lv ZZ, Tu Y, Tu ST (2018) Research on Shear Horizontal Waves in Bars of Rectangular Cross-Section. J Material Sci Eng 7: 486. doi: 10.4172/2169-0022.1000486

The propagating theoretical equation of SH waves in waveguide bars is derived in Section 2. The wave structure of SH waves is analyzed in Section 3. The waves in a series of bars with different structural sizes and different materials are analyzed via the ANSYS software and experiments in Section 5. Results and discussions are provided to validate the simulated results in Section 6, followed by conclusions in Section 6.

Propagating Theoretical Equation of SH Waves

Materials of waveguide bars are normally selected as the same materials with the specimens according to the theory about the transmission and reflection of ultrasonic waves [28]. For high temperature components applied in aerospace and process industries, isotropic materials are generally applied, so the materials of waveguide bars are selected as isotropic materials.

For any isotropic medium, the particle displacement field $u(x, t)$ should satisfy Navier's displacement equations of motion [29]:

$$\mu\nabla^2 u(x,t)+(\lambda+\mu)\nabla\nabla\bullet u(x,t)=\rho\frac{\partial^2 u(x,t)}{\partial t^2} \tag{1}$$

Let's firstly assume that the width of the waveguide bar is wide enough, and the bar can be considered as an infinite plate on this condition. Because the particle displacements caused by any of the SH waves are in a plane which is parallel to the surfaces of the bar, as shown in Figure 1. The waves propagate in the x direction and the particles vibrate in the y direction. The displacement vectors have only a y component i.e, $u_x(x, t)=u_z(x, t)=0$ and the y component can be specified as [30]

$$u_y(x,z,t)=f(z)e^{i(kx-\omega t)} \tag{2}$$

Where k is the wavenumber of the mode and ω is circular frequency. This equation represents waves propagating along the x-coordinate direction and wave motions have a fixed distribution in the z-coordinate direction.

If only the u_y component of the particle displacement is nonzero, and u_y is independent of y, then eqn. (1) reduces to

$$\frac{\partial^2 u_y(x,z,t)}{\partial x^2}+\frac{\partial^2 u_y(x,z,t)}{\partial z^2}=\frac{1}{c_T^2}\frac{\partial^2 u_y(x,z,t)}{\partial t^2} \tag{3}$$

Where $c_T^2=\mu/\rho$.

Substituting eqn. (2) into eqn. (3) results in

$$\frac{\partial^2 f(z)}{\partial z^2}+\left(\frac{\omega^2}{c_T^2}-k^2\right)f(z)=0 \tag{4}$$

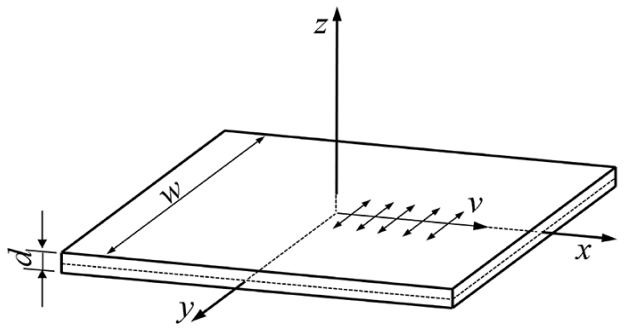

Figure 1: SH waves propagating in a waveguide bar of rectangular cross-section.

This equation has the general solution

$$f(z)=\mathrm{A}\sin(qz)+\mathrm{B}\cos(qz) \tag{5}$$

where q is defined as

$$q=\sqrt{\frac{\omega^2}{c_T^2}-k^2} \tag{6}$$

and A and B are arbitrary constants. Therefore, the general form of the displacement field is

$$u_y(x,z,t)=\left[\mathrm{A}\sin(qz)+\mathrm{B}\cos(qz)\right]e^{i(kx-\omega t)} \tag{7}$$

$$=\sqrt{\mathrm{A}^2+\mathrm{B}^2}\sin(qz+\varphi)e^{i(kx-\omega t)},$$

where $\varphi=\arccos\left(\mathrm{A}/\sqrt{\mathrm{A}^2+\mathrm{B}^2}\right)$. Eqn. (7) is a bounded function, and its boundary is:

$$\left|u_y(x,z,t)\right|=\sqrt{\mathrm{A}^2+\mathrm{B}^2} \tag{8}$$

Normally, the amplitude of the wave vibration is distinctly small relative to the mechanical structure of the waveguide bar. That is,

$$w\gg\left|u_y(x,z,t)\right|=\sqrt{\mathrm{A}^2+\mathrm{B}^2} \tag{9}$$

and the waves propagate only along the x-coordinate direction. Therefore, the SH waves can propagate in a waveguide bar of rectangular cross-section just like how they propagate in an infinite plate.

Wave Structure Analysis of SH Modes

When we separate the total displacement field into symmetric and anti-symmetric components with respect to z, eqn. (7) can be rewritten as

$$u_y^s(x,z,t)=B\cos(qz)e^{i(kx-\omega t)} \tag{10}$$

$$u_y^a(x,z,t)=A\sin(qz)e^{i(kx-\omega t)}$$

The superscript s denotes a symmetric mode and a denotes an antisymmetric mode.

The tractions-free boundary conditions at the upper and lower plate surfaces yield

$$\tau_{zy}(x,z,t)\big|_{z=\pm\frac{d}{2}}=0 \tag{11}$$

The traction component τ_{zy} is given by [31]:

$$\tau_{zy}=u\frac{\partial u_y}{\partial z} \tag{12}$$

Substituting of eqn. (10) into eqn. (12) yields

$$\tau_{zy}(x,z,t)=-\mu qB\cos(qz)e^{i(kx-\omega t)} \text{ for symmetric modes} \tag{13a}$$

and

$$\tau_{zy}(x,z,t)=\mu qA\sin(qz)e^{i(kx-\omega t)} \text{ for antisymmetric modes} \tag{13b}$$

Substituting of eqn. (13) into boundary conditions eqn. (11) yields the dispersion equations

$$\cos(qz)=0 \text{ for symmetric modes} \tag{14a}$$

and

$$\sin(qz)=0 \text{ for antisymmetric modes} \tag{14b}$$

The roots of eqn. (14) are

$$qz=n\pi/2 \tag{15}$$

where $n \in \{0,2,4,...\}$ for symmetric SH modes and $n \in \{1,3,5,...\}$ for antisymmetric SH modes.

Euler transformation of exponential function in eqn. (10) yields

$$e^{i(kx-\omega t)} = \cos(kx-\omega t) + i\sin(kx-\omega t) \tag{16}$$

Substituting of eqn. (16) into eqn. (10) yields

$$\begin{aligned} u_y^s(x,z,t) &= B\cos(qz)\cos(kx-\omega t) + iB\cos(qz)\sin(kx-\omega t) \\ u_y^a(x,z,t) &= A\sin(qz)\cos(kx-\omega t) + iA\sin(qz)\sin(kx-\omega t) \end{aligned} \tag{17}$$

Using the form of q given in eqn. (15) and taking the real parts of eqn. (17), the displacement fields of the symmetric and antisymmetric SH modes can be written as

$$\begin{aligned} u_y^s(x,z,t) &= B\cos(n\pi z/d)\cos(kx-\omega t) \\ u_y^a(x,z,t) &= A\sin(n\pi z/d)\cos(kx-\omega t) \end{aligned} \tag{18}$$

Because the wavenumber $k = \omega/c$ and time $t = x/c$, $\cos(kx-\omega t)=1$ That is to say that variable x represents only the direction of wave propagation. Therefore, eqn. (18) can be changed to

$$\begin{aligned} u_y^s(x,z,t) &= B\cos(n\pi z/d) \\ u_y^a(x,z,t) &= A\sin(n\pi z/d) \end{aligned} \tag{19}$$

Note that the variation of fields of SH modes across the thickness of plate do not vary along any mode's dispersion curve. Sketches of the zeroth, first, second, and third SH modes are given in Figure 2, the displacement amplitude of which is normalized. w^S represents symmetric modes and w^A represents antisymmetric modes. It is worth noting that the displacement field of the SH0 mode guide wave remains uniform in the thickness direction.

Verification of the SH0 Wave Propagating in Waveguide Bars

Introduction of the simulation and experiment system

In order to find a universal conclusion for bars to propagate SH0 wave, the curves of wave velocities versus widths are analyzed by both the finite element method using ANSYS software and the experimental method, because wave velocities change when waves are interfered by boundaries. Moreover, three kinds of materials are selected aiming at deriving a universal design formula. They are 316L stainless steel, aluminum and copper. The parameters of these materials are listed in Table 1.

According to eqn. (20) of the wavelength [26], some wavelengths can be calculated for the normally used frequency 1 MHz and 2 MHz, and they are enumerated in Table 2.

$$\lambda = \frac{C_T}{f} \tag{20}$$

Where λ is the wavelength, and f is the excitation frequency.

During simulation, the excitation displacement distributes uniformly in the thickness direction, which is similar with the displacement wave structure of SH0 wave in above-mentioned Figure 2a in section 3. The excitation signal is 10-cycle sinusoidal displacement tone burst modulated by a Hanning window with a center frequency f_c. In the present research f_cs are chosen as 1 MHz and 2 MHz, respectively. The excitation signal is applied on one end of the waveguide bar, and the reception signal is picked up on the same end. The waveguide bar is modeled using the SOLID 164 element.

Moreover, the experimental system is setup and shown in Figure 3. It includes a signal generator (Tektronix, AFG 3021C), a mixed signal oscilloscope (Tektronix, MDO 3012), a power amplifier (AG 1006), a duplexer (Ritec, RDX-6), and two transducers (Olympus V153-RM). The central frequencies of the transducers are 1 MHz and 2 MHz. Ten cycles sinusoidal tone bursts modulated with a Hanning window are generated at 1 MHz and 2 MHz, respectively. Signals are recorded at a sampling rate of 50 MHz. A purpose-made installation tool is applied to fix the transducer on one end of the waveguide bar. During testing, the transducer works as both exciter and receiver.

Materials	Density (kg/m³)	Elastic modulus (Gpa)	Poisson's ratio	Bulk shear wave speeds C_T (m/s)
316L	7800	211	0.286	3242
Aluminum	2700	71	0.33	3144
Copper	8800	123	0.35	2274

Table 1: The parameters of the materials.

Materials of the plate	1 MHz			2 MHz		
	λ	5λ	6λ	λ	5λ	6λ
316L	3.24 mm	16.2 mm	19.44 mm	1.62 mm	8.1 mm	9.72 mm
Aluminum	3.14 mm	15.7 mm	18.84 mm	1.57 mm	7.85 mm	9.42 mm
Copper	2.27 mm	11.35 mm	13.62 mm	1.14 mm	5.7 mm	6.84 mm

Table 2: The wavelengths of three different materials.

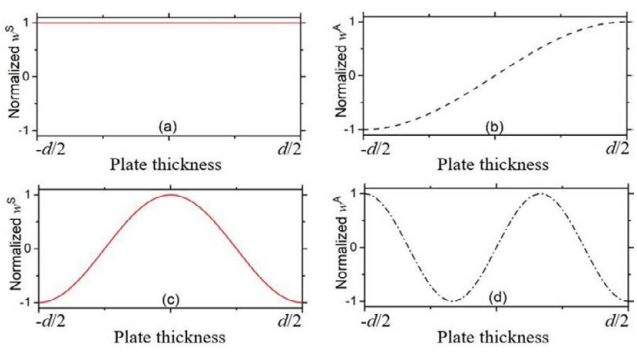

Figure 2: The displacement wave structure of SH waves: (a) SH0 mode; (b) SH1 mode; (c) SH2 mode; (d) SH3 mode.

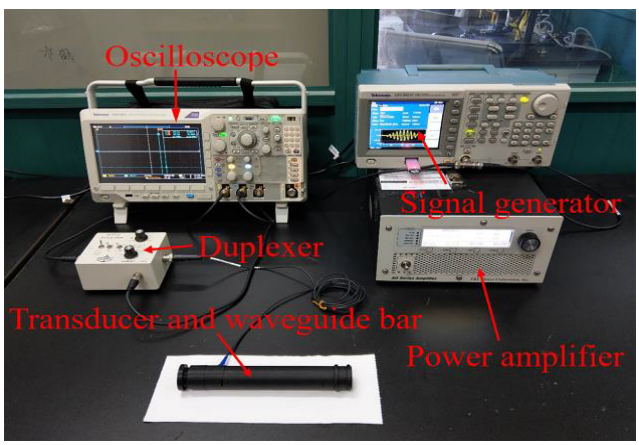

Figure 3: Experimental system.

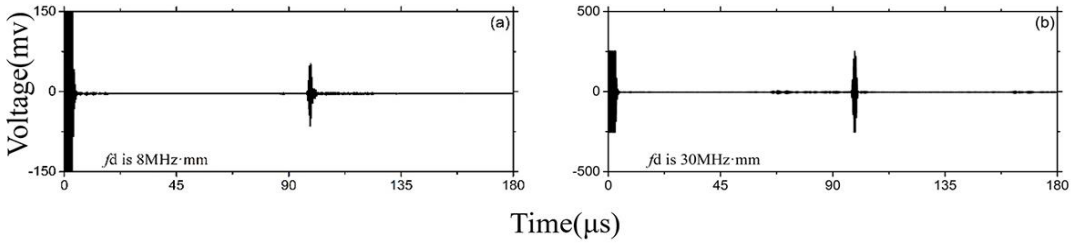

Figure 4: Waveforms propagation in 316L stainless waveguide bars with different thicknesses (Experimental frequency is 2 MHz).

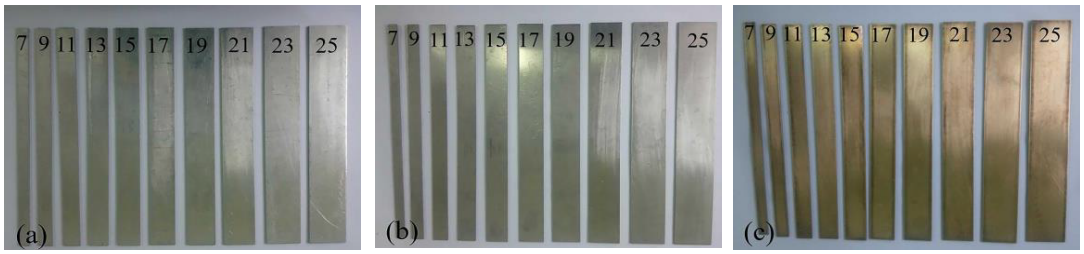

Figure 5: The specimen bars made of different materials: (a) 316L stainless bars; (b) aluminum bars; (c) copper bars.

Thickness analysis

According to the theory of the wave structure, it is known that SH0 wave is independent of thickness. And the loading style is similar with the SH0 wave structure when we install sensors on one end of the bar. Two bars made of 316L stainless are designed to verify the effect of thickness. Their width is 15 mm, and their length is 150 mm. Their thickness are 4 mm and 15 mm, respectively.

The simulated and experimental waveforms propagating through bars at 2 MHz frequency are alike. They are non-dispersive. The experimental waveforms are plotted in Figure 4. The wave is SH0 mode judging by speed. Therefore, it can conclude that the thickness of bars is independent to excite the SH0 wave.

Width analysis

Based on the thickness analysis, the thickness of bars is selected as 1 mm to the convenience of choosing material. Some waveguide bars are fabricated, and their pictures are shown in Figure 5. The widths are different, which are odds in the range from 7 mm to 25 mm.

The group velocity dispersions are analyzed at two different excitation frequencies. The experimental phenomena coincide very well with the simulation results. Comparing the critical width with Table 2, it is found that the group velocities depend on the width of the bars when the width is narrower than their critical values 6λ and they become width independent when the width is wider than 6λ. The curves of group velocity dispersions versus widths of waveguide bars at 1 MHz are depicted in Figure 6. The group velocity increases monotonously. And it approaches asymptotically the bulk shear velocity C_T at the critical width.

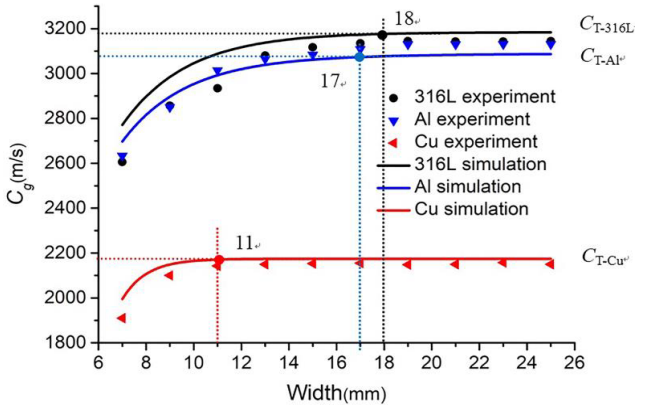

Figure 6: SH mode group velocity dispersion curves in waveguide bars (Experimental frequency is 1 MHz).

Conclusions

In order to study the propagation characteristics of the shear horizontal waves in waveguide bars of rectangular cross-section, the wave propagation equation of SH waves in waveguide bars is derived firstly. The wave equation describes a bounded monotone function, which demonstrates the SH waves can propagate in waveguide bars just like in an infinite plate. Secondly, the wave structure is analyzed. It is found that the SH0 wave is independent of thickness. And the loading style is designed based on SH0 wave structure. Then SH waves propagating in waveguide bars are analyzed by ANSYS simulation and experiment. Results show that the waves propagate uniquely along the length direction, and the waveform is independent of the thickness. Moreover, it is also found that the non-dispersive wave in a form of SH0 mode can propagate in bars when their width is bigger than 6λ of any waveguide material. Therefore, the conclusion can be drawn that the SH waves can propagate in waveguide bars of rectangular cross-section like in infinite plate when widths and thicknesses of bars satisfy the critical values.

References

1. Zhang HC, Jia JH, Wang N, Hu XY, Tu ST, et al. (2013) Development of on-line monitoring systems for high temperature components in power plants. Sensors 13: 15504-15512.

2. Qiu L, Yuan, SF, Chang FK, Bao Q, Mei H (2014) On-line updating Gaussian

mixture model for aircraft wing spar damage evaluation under time-varying boundary condition. Smart Mater. Struct 23: 125001.

3. Cawley P (2018) Structural health monitoring: Closing the gap between research and industrial deployment. Struct Health M pp: 1-20.
4. Vasiljevic M, Kundu T, Grill W, Twerdowski E (2008) Pipe Wall Damage Detection by Electromagnetic Acoustic Transducer Generated Guided Waves in Absence of Defect Signals. Journal of the Acoustical Society of America 123: 2591-2597.
5. Ahmad R, Banerjee S, Kundu T (2009) Pipe Wall Damage Detection in Buried Pipes Using Guided Waves. Journal of Pressure Vessel Technology 131: 011501.
6. Teo YH, Chiu WK, Chang FK (20098) Optimal placement of sensors for sub-surface fatigue crack monitoring. Theoretical and applied fracture mechanics 52: 40-49.
7. Burrows SE, Fan Y, Dixon S (2014) High temperature thickness measurements of stainless steel and low carbon steel using electromagnetic acoustic transducers. NDT&E Int 68: 73-77.
8. Xiang YX, Deng MX, Xuan FZ (2014) Creep damage characterization using nonlinear ultrasonic guided wave method: a mesoscale model. Journal of Applied Physics 115: 044914.
9. Li FC, Liu ZG, Sun XW (2015) Propagation of guided waves in pressure vessel. Wave Motion 52: 216-228.
10. Xiang YX, Zhu WJ, Liu CJ, Xuan FZ, Wang YN, et al. (2015) Creep degradation characterization of titanium alloy using nonlinear ultrasonic technique. NDT&E Int 72: 41-49.
11. Jen CK, Legoux JG, Parent L (2000) Experimental evaluation of clad metallic buffer rods for high temperature ultrasonic measurements. NDT & E Int 33: 145-153.
12. Hayashia T, Song WJ, Rose JL (2003) Guided wave dispersion curves for a bar with an arbitrary cross-section, a rod and rail example. Ultrasonics 41: 175-183.
13. Gan C, Wei Y, Yang S (2014) Longitudinal wave propagation in a rod with variable cross-section. Journal of Sound and Vibration 333: 434-445.
14. Cheong YM, Kim KM, Kim DJ (2017) High-temperature ultrasonic thickness monitoring for pipe thinning in a flow-accelerated corrosion proof test facility. Nuclear Engineering and Technology 49: 1463-1471.
15. Heijnsdijk AM, Klooster JMV (2002) Ultrasonic waveguide. U.S. Patent 6400648, June 4.
16. Lynnworth LC, Liu Y, Umina JA (2005) Extensional bundle waveguide techniques for measuring flow of hot fluids. IEEE transactions on ultrasonics, ferroelectrics, and frequency control 52: 538-544.
17. Kwon YE, Jeon HJ, Kim HW, Kim YY (2014) Waveguide tapering for beam-width control in a waveguide transducer. Ultrasonics 54: 953-960.
18. Cegla FB, Cawley P, Allin J, Davies J (2011) High-temperature (>500℃) wall thickness monitoring using dry-coupled ultrasonic waveguide transducers. IEEE Trans. Ultrason. Ferroelectr. Control 2011; 58(1): 156-167.
19. Cegla FB (2008) Energy concentration at the center of large aspect ratio rectangular waveguides at high frequencies. J Acoust Soc Am 123: 4218-4226.
20. Jia JH, Wang QY, Liao ZY, Tu Y, Tu ST (2017) Design of waveguide bars for transmitting a pure shear horizontal wave to monitor high temperature components. Materials 10: 1027.
21. Kamal A, Giurgiutiu V (2014) Shear horizontal wave excitation and reception with shear horizontal piezoelectric wafer active sensor (SH-PWAS). Smart Mater Struct 23: 085019.
22. Köhler B, Gaul T, Lieske U, Schubert F (2016) Shear horizontal piezoelectric fiber patch transducers (SH-PFP) for guided elastic wave applications. NDT&E International 82: 1-12.
23. Seung HM, Park C, Kim YY (2016) An omnidirectional shear-horizontal guided wave EMAT for a metallic plate Original research article. Ultrasonics 69: 58-66.
24. Zhou WS, Li H, Yuan FG (2014) Guided wave generation, sensing and damage detection using inplane shear piezoelectric wafers. Smart Mater Struct 23: 015014.
25. Miao HC, Huan Q, Li FX (2016) Excitation and reception of pure shear horizontal waves by using face-shear d24 mode piezoelectric wafers. Smart Mater Struct 25: 11LT01.
26. Miao HC, Dong SX, Li FX (2016) Excitation of fundamental shear horizontal wave by using face-shear (d36) piezoelectric ceramics. Journal of Applied Physics 119: 2571.
27. Mindlin RD, Fox EA (1960) Vibrations and waves in elastic bars of rectangular cross section. Journal of Applied Mechanics 27: 1.
28. Du GH, Zhu ZM, Gong XF (2012) Fundamentals of Acoustics [M]. Nanjing, Nanjing University Press.
29. Malvern LE (1969) Introduction to the mechanics of a continuous medium [M]. Englewood cliffs, N J: Prentice-Hall.
30. Rose JL (1999) Ultrasonic Waves in Solid Media [M]. New York, Cambridge University Press.
31. Victor G, Yuan SF (2017) Structural health monitoring with piezoelectric water active sensors [M]. Science Press.